17th World Conference on Earthquake Engineering, 17WCEE
Sendai, Japan - September 13th to 18th 2020

CYCLIC TESTING AND NUMERICAL MODELING FOR COMBINED AND CONFINED MASONRY WALLS

J. E. Mayorga[1,2], A. Tena-Colunga[3], N. Domínguez[4], H. I. Archundia-Aranda[5]

[1] First Captain Engineer, Secretaría de la Defensa Nacional, Dirección General de Educación Militar y Rectoría de la U.D.E.F.A., Av. México-Tacuba S/No., Col. Popotla, 11400 Mexico City, MEXICO, e-mail: mayorga.edmundo@gmail.com
[2] PhD. Candidate, Posgrado en Ingeniería Estructural, Universidad Autónoma Metropolitana-Azcapotzalco, Av. San Pablo 180, Col. Reynosa Tamaulipas, 02200 Mexico City, MEXICO, e-mail: al2153800538@azc.uam.mx
[3] Professor, Departamento de Materiales, Universidad Autónoma Metropolitana Azcapotzalco, Av. San Pablo 180, Col. Reynosa Tamaulipas, 02200 Mexico City, MEXICO, e-mail: atc@correo.azc.uam.mx
[4] Professor, Escuela Superior de Ingeniería y Arquitectura (ESIA), Instituto Politécnico Nacional Unidad Zacatenco, Av. Instituto Politécnico Nacional s/n, esquina Av. Wilfrido Massieu, Col. San Pedro Zacatenco, 07738 Mexico City, MEXICO, e-mail: ndominguez@ipn.mx
[5] Professor, Departamento de Materiales, Universidad Autónoma Metropolitana Azcapotzalco, Av. San Pablo 180, Col. Reynosa Tamaulipas, 02200 Mexico City, MEXICO, e-mail: archundia@correo.azc.uam.mx

Abstract

Masonry construction is widely used in Mexico and other countries for lowrise housing and buildings, thanks to its advantages in initial costs (commonly cheaper than reinforced concrete), as well as its ease of construction and availability of cheap workmanship in most cases. A variation of an ancient tradition from the construction practice of the Colonial period of Mexican history, named "*combined masonry*", has been recently retaken and updated in Mexico. This structural system is being built using a hybrid combination of layers of concrete blocks mixed with layers of clay bricks, increasing the uncertainty of the expected elastic and inelastic mechanical behavior. This structural system is currently known as "*combined and confined masonry*".

An experimental program to evaluate the cyclic behavior of combined and confined masonry walls is reported, as well as the corresponding progress in numerical modeling. In this sense, experimental tests in masonry units and mortar were carried out to obtain index properties and constitutive stress-strain curves for each material. In addition, small combined masonry subassemblies tested in compression and diagonal compression were used to obtain their corresponding stress-strain curves and define index properties such as the compressive strength $f_m^{'}$, Young's modulus E_m, shear strength $v_m^{'}$ and the shear modulus G_m. All tests were carried out according to the Mexican masonry design guidelines.

To evaluate the earthquake-resistant for this structural system, the cyclic testing of two combined and confined walls scale was performed using the protocol established in the Mexican guidelines for masonry structures. The internal instrumentation consisted of 36 strain gauges attached to the steel longitudinal and transversal reinforcement of the confining elements. The external instrumentation was composed of five LVDT. Nonlinear analyses of both small combined masonry subassemblies and the cyclic testing combined and confined masonry walls have been carried out, using simple models and detailed finite element models where the experimentally obtained constitutive stress-strain curves are used. Obtained results are discussed for each modeling in terms of how successful were they to reproduce the global response envelope.

Keywords: Combined and confined masonry; experimental tests; damage modeling; nonlinear finite element analysis

1. Introduction

Masonry is a construction material widely used in Mexico and other countries to build lowrise housing buildings, thanks to its advantages in cost (commonly cheaper than concrete), as well as its ease of construction in most of the cases. However, the mechanical modeling of masonry under cyclic loads could be rather complex, due to the heterogeneity of their components (bricks, mortar joints, tie-beams and tie-columns, steel reinforcement, etc) associated to the traditional practices of construction [1, 2].

An ancient tradition from the construction of the Colonial period of Mexican history, named "*combined masonry*", has been recently retaken and updated in Mexico. In recent decades many structures with masonry walls are being built using a hybrid combination of concrete blocks and layers of clay bricks, increasing the uncertainty of the elastic and inelastic mechanical behavior. This structural system is currently known as "*combined and confined masonry*" [2].

It is well known that standard masonry is non-homogeneous and anisotropic, with an "elastic" range very limited in comparison to other building materials, including concrete. Multiple efforts have been done to develop some orthotropic and anisotropic formulations according to the particular behavior observed in experiments, particularly for concrete. In masonry, however, there are just limited studies in this regard and there is not enough experimental evidence oriented to model orthotropic behavior to recommend the implementation of some of these formulations or even to identify specific parameters to use into these models for common analysis and design of masonry structures [3]. For these reasons, an experimental campaign was started to assess these parameters and, in parallel, evaluate the adaptation of a nonlinear isotropic damage model proposed for concrete to masonry for numerical simulations.

The research strategy was organized as follows:

a) Execution of an experimental program applied for obtaining parameter values required in the numerical models;
b) Selection of suitable numerical models to represent the mechanical behavior of masonry;
c) Calibration of the numerical models with the experimental test and,
d) Comparison of the experimental results with numerical models.

2. Experimental program

The experimental program was oriented to obtain index properties to use for modeling and design purposes. In this sense, tests in masonry units, short columns, wallets and walls scale 1:1 was done according with the Mexican masonry guidelines [4, 5, 6, 7, 8, 9].

2.1 Test for blocks, bricks and mortar

Experimental tests in masonry units and mortar were carried out (Fig. 1) to obtain index properties and the maximum stress and deformation associated to it. The index properties for blocks, bricks and mortar are summarized in Table 1.

(a) (b) (c)

Fig. 1 – Experimental tests in: a) blocks, b) brick and, c) mortar

According with the masonry Mexican code, the compressive design masonry strength, $f_p^{'}$, should be calculated as:

$$f_p^{'} = \frac{\overline{f_p}}{1+2.5c_p} \qquad (1)$$

where $\overline{f_p}$ is the average compressive strength and c_p is the coefficient of variation of such tests. According to Mexican masonry guidelines, a minimum of nine specimens are required to assess any nominal masonry property.

Table 1 – Index properties for blocks, bricks and mortar

Property	Blocks	Bricks
Volumetric weight (ton/m^3)	1.58	1.35
Absorption	6.38	24.89
Initial rate of absorption (gr/min)	17.02	24.81
Saturation coefficient	0.88	0.84
Compressive strength		
Mean $\overline{f_p}$ (MPa)	16.5	7.6
Design $f_p^{'}$ (MPa)	11.0	4.0
Mean deformation	0.0136	0.073
Young's Modulus (MPa)	2,070	434

The index properties for the mortar used (mortar type I according to Mexican Guidelines) are summarized in Table 2. In accordance with the code, cubes of 5 cm by side were tested in simple compression to determine the compressive strength of the mortar (Fig. 1c).

Table 2 – Index properties for mortar type I

Property	Mortar
Volumetric weight (ton/m^3)	1.80
Compressive strength	
Mean $\overline{f_j}$ (MPa)	20.5
Design $f_j^{'}$ (MPa)	14.0
Mean deformation	0.0181

2.2 Analytical expressions to obtain stress-strain curve

Few experimental programs report stress-strain curves for masonry components (in particular, masonry units and mortars) because at the time of reporting the results of experimental tests, commonly only peak strength or stress values are reported, mainly in compression.

To the author's knowledge, few researchers have proposed equations to define the stress-strain curve for brittle materials such as masonry units or mortar. Popovics [10] proposed in 1973 a series of expressions to represent these curves, although validated in experimental tests to compression of concrete and mortar cylinders. In the proposed equations by Popovics (Eqs. 2 to 5) f is the axial stress, ε the strain caused by f, f_0 is the ultimate stress, ε_0 is the ultimate strain, E is Young's modulus and n is a parameter that depends of the material which was tested (concrete, mortar or "paste"). Popovics expressions are:

- when the strength and ultimate deformation are obtained experimentally:

$$f = f_o \frac{\varepsilon}{\varepsilon_o}\left(\frac{n}{n-1+\left(\varepsilon/\varepsilon_o\right)^n}\right) \tag{2}$$

- when only the ultimate strength f_0 is experimentally obtained. The expression is similar to equation 2, in this case the ultimate deformation value is calculated as:

$$\varepsilon_o = 0.00027 * \sqrt[4]{f_o} \tag{3}$$

- when the modulus of elasticity is obtained experimentally.

$$f = E\varepsilon\left(\frac{n-1}{n-1+\left(\varepsilon/\varepsilon_o\right)^n}\right) \tag{4}$$

- the parameter n is assessed as follows, depending on the material used:

$$\begin{aligned} n_{concrete} &= 0.4E - 3f_0 + 1.0 \\ n_{mortar} &= 0.15E - 3f_0 + 1.5 \\ n_{pasta} &= 12 \end{aligned} \tag{5}$$

From the tests carried out in concrete masonry units, some parameters had to be adjusted to the generic curves defined by Popovics equations. Therefore, the obtained n parameter for our tested concrete masonry units and mortar are given in Eq. 6. The obtained correlation between experimental curves and adjusted Popovics equations are shown in Fig. 2.

$$\begin{aligned} n_{concrete} &= 0.15 f_0 \\ n_{mortar} &= 0.06 f_0 \end{aligned} \tag{6}$$

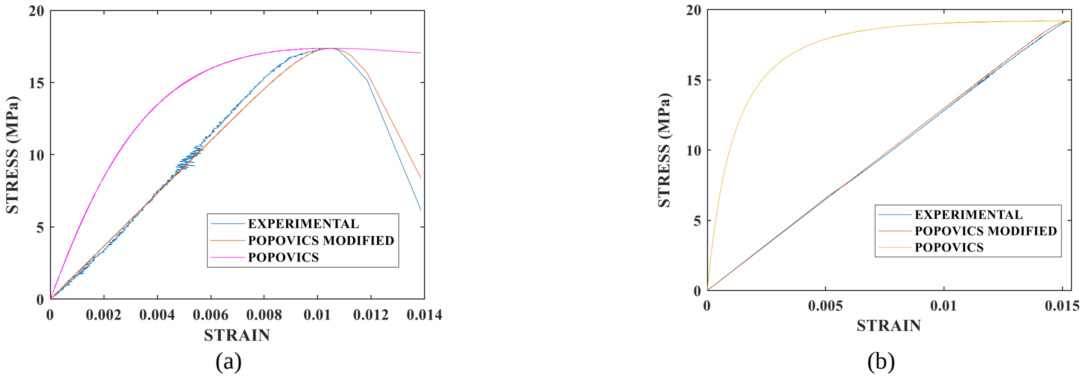

Fig. 2 – Comparision of stress-strain curves, (a) mortar cubes and (b) concrete blocks

2.3 Test of prisms and wallets

Nine combined masonry prisms were constructed to estimate the compressive strength and Young's modulus for the combined masonry. The instrumentation was composed by two LVDT in each side of the prism (Fig. 3a). The mode of failure is shown in Fig. 3b, where the clay bricks failed by crushing. It is worth noting that no cracks were observed in the concrete blocks, due to the higher compressive strength compared to the corresponding clay bricks. Tests were carried out according to the guidelines and requirements provided by NTCM-2017 [4]. Bed and head joints were filled with mortar type I. Tests results are summarized in Table 3.

To calculate f'_m the C_m obtained experimentally was used, the minimum value established in NTCM-2017 is 0.15.


(a)


(b)

Fig. 3 – Combined masonry prism arrangements, (a) instrumentation and (b) mode of failure.

Table 3 – Index properties for combined masonry prisms

Mean $\overline{f}_m$ (MPa)	4.8
C_m	0.164
Design f'_m (MPa)	3.4
Young's modulus (MPa)	2,840
Mean deformation	0.005991

Nine combined masonry wallets were constructed to estimate an indirect shear strength (diagonal tension) and the shear modulus G_m, the instrumentation was composed by four LVDT two in each side of the wallets (Fig. 4a); in Fig. 4b the failure mechanism is depicted where the mode of failure was by diagonal tension. The tests were carried out according to the guidelines and requirements provided by NTCM-2017 [4]. Bed and head joints were filled with mortar type I. The results are summarized in Table 4. $C_v = 0.20$ was used as this is the minimum value established to be used to assess v'_m in NTCM-2017.

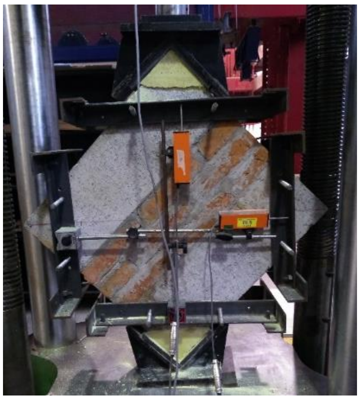
(a)


(b)

Fig. 4 – Combined masonry wallets arrangement, (a) instrumentation and (b) mode of failure

2.4 Test of combined and confined masonry walls at scale 1:1.

Two walls were constructed and tested under cyclic lateral load, the code for identifying each wall was MMCC-*i*, where *i* is the index to identify the number of wall sequentially tested. The tested walls are shown in Fig. 5. The internal and external instrumentation are depicted in Fig. 6. The internal instrumentation consisted of 36 strain gauges attached to the steel longitudinal and transversal reinforcement of the confining elements (Fig. 6a). The external instrumentation (Fig. 6b) was composed of five LVDT.

Table 4 – Index properties for combined masonry wallets

Mean $\bar{v}_m$ (MPa)	0.70
C_v obtained experimentally	0.160
Design $v_m^{'}$ (MPa)	0.467
Shear modulus (MPa)	324.90
Mean deformation	0.002074

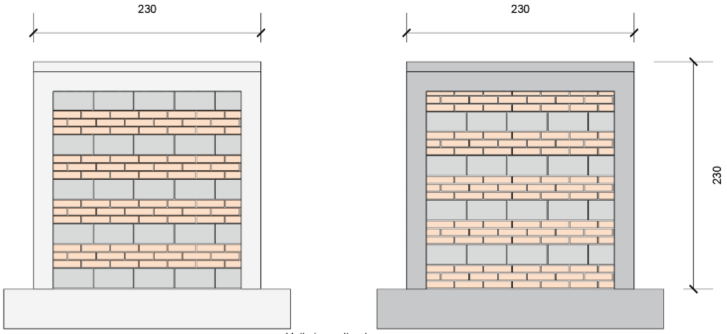

(a) MMCC-*1* (b) MMCC-*2*

Fig. 5 – General geometry of tested confined and combined masonry walls

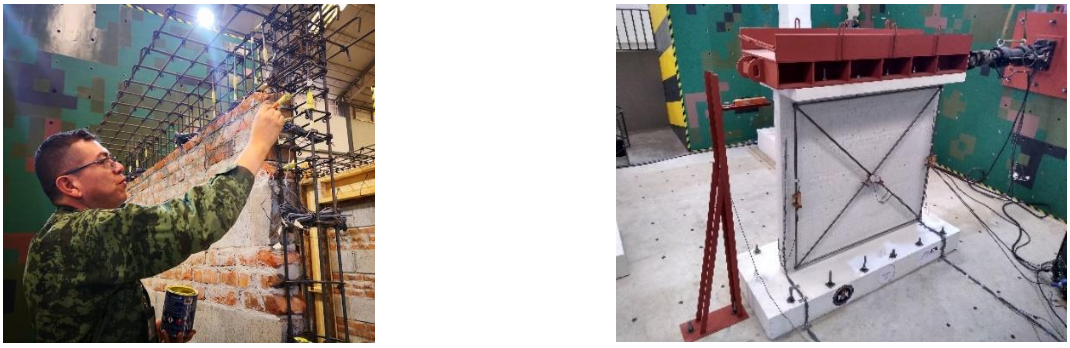
(a) Internal instrumentation (b) External instrumentation

Fig. 6 – Instrumentation for the confined and combined masonry walls

Confining tie-column elements were 12x20 cm and the confining rectangular bond-beam was 12x30 cm, a slab portion of 10x80 cm was casted at the top of the confining bond-beam. The compressive strength of the concrete used for the confining elements was specified as $f_c^{'} = 150\ kg/cm^2\ (14.7\ MPa)$. The testing of the walls was done in the new reaction floor and reaction wall of the Engineering Military College belonging to the Mexican Army. A special steel beam was designed to apply uniformly distributed vertical loading of 1.4 ton/m (13.7 kN/m) and to help applying with the actuator the cyclic lateral loading.

The cycling testing of the walls was done following the general guidelines of Appendix A of NTCM-2017 [4] required for earthquake-resistant masonry walls systems. According to the testing protocol of reference, masonry walls must be subjected to repeated cycles at least 25%, 50% and 100% the estimated cracking load for the walls, in Fig. 7 the load control is shown.

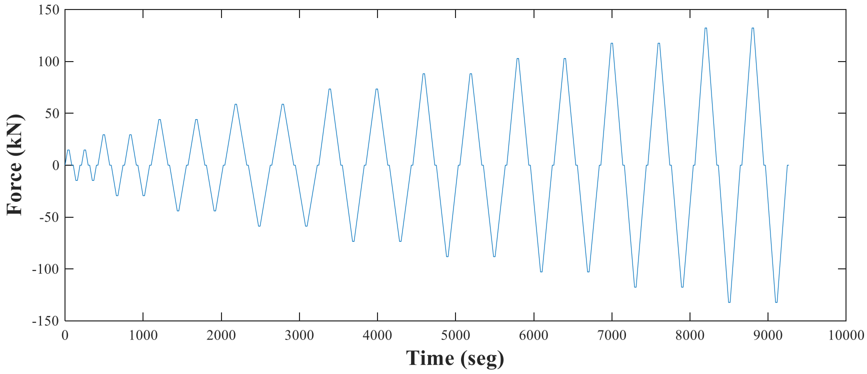

Fig. 7 – Cyclic loading sequence

The hysteretic loops obtained for each wall from the cyclic testing protocol are depicted in Fig. 8. During the testing of walls, in specific during the negatives cycles (pulling), the displacement recorded was not the same that in the positive cycles (pushing), that is the reason of the asymmetric loops. In Fig. 8a, in the blue-dotted line it is shown the envelope for wall MMCC-1. In Figs 9a and 9b the cracking pattern is shown. During the testing of wall MMCC-2, when 50 kN was reached, occurred an unexpected out-plane failure of the wall, due to a small accidental eccentricity between the axis of the actuators and the corresponding axis of wall, which was not obvious before the texting but it was confirmed using a theodolite afterwards, as a small eccentricity existed between the centerline of the circular holes of the reaction floor and the centerline of the holes were the actuators were installed. In Figs. 10a and 10b the failure mechanism out-plane and cracking are depicted. This resulting was interesting however, as it demonstrates how vulnerable are unbraced confined masonry walls out-of-plane when the lateral load is applied with a small eccentricity in their plane and then, after initial cracking, bending moments out of plane lead the walls to collapse.

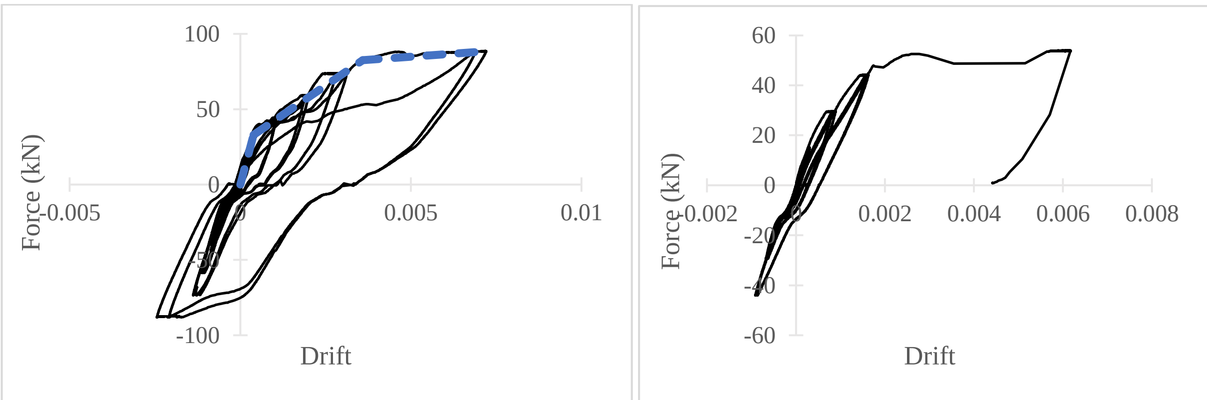

(a) Wall MMCC-1 (b) Wall MMCC-2

Fig. 8 – Hysteric loops for the tested confined and combined masonry walls.

3. Numerical models

3.1 Mazar's damage model

To represent the microstructural damage that can occur in the masonry units, mortar and confining elements, the continuum damage model of Mazars was selected. This model was originally proposed for the study of concrete structures, and recently it has been employed for the analysis of masonry structures, since both materials exhibit a fragile behavior [11].

In order to perform numerical analyses, FEAP program [12] was used, a free and open-source Finite Element code with a wide number of nonlinear material models included, which allow the modeling of different materials, mainly concrete and steel. For the linear and nonlinear modeling of masonry walls, 2D solid elements were used, combined with Mazars' damage model.

To describe the evolution of the damage, the Mazars' damage model requires in total eight parameters [13]: the two elastic coefficients E and v, and six dimensionless values A_t, B_t, A_c, B_c, ε_{d0} and k. Parameters A and B are used to represent the quasi-fragile behavior in traction and the classical concrete behavior in compression, allowing to modulate the shape of the curve post-peak; ε_{d0} is the threshold deformation damage and k introduces an horizontal asymptote in pure shearing on stress-strain curve.

(a) (b)

Fig. 9 – Wall MMC-1, (a) Cracking at expected nominal shear load (88.3 kN) and, (b) Final cracking pattern at 112.8 kN

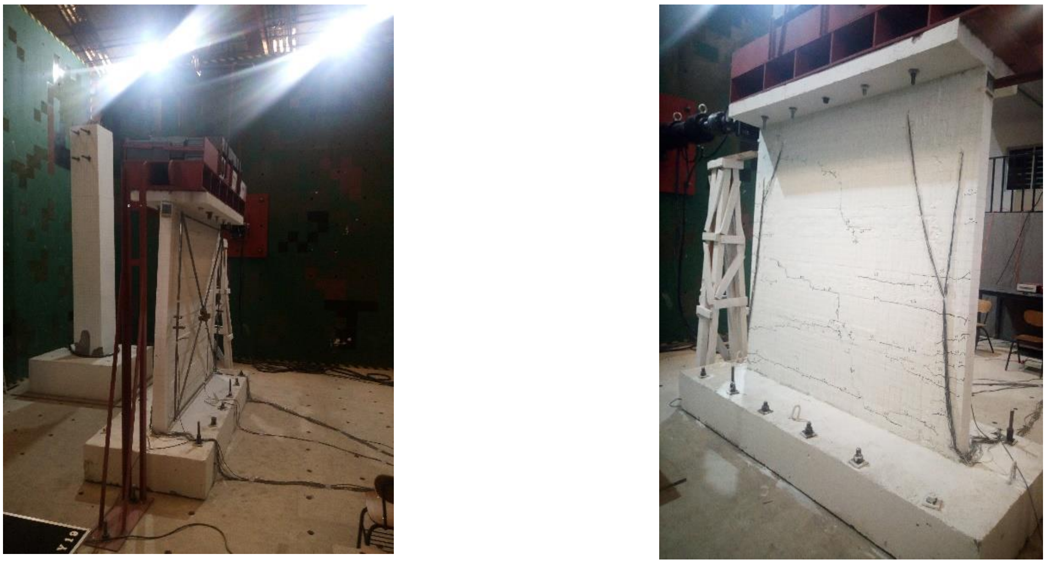

(a) (b)

Fig. – 10 Wall MMCC-2 (a) Out-plane failure and, (b) Final cracking patterns of tested wall

In Mazars' damage model, two parameters are included to control the damage in the continuum; D_t associated to a tension and D_c associated to the damage under compression. The process of damage starts when the equivalent strain reaches the threshold [14].

3.2 Numerical models of prisms and wallets

For modeling combined masonry prisms and wallets, the dimensions and mechanical properties described in Figs. 3 and 4 and Tables 3 and 4 were considered. Solids elements in 2D (QUAD4) were used. The boundary conditions and the corresponding finite element mesh are depicted in Figs. 11 and 12. For prisms, 529 elements were used and for wallets 900 elements. As a practical numerical approximation, both models were considered homogeneous (of course, combined masonry is not) and were controlled by displacement. The obtained experimental and numerical curves for prisms and wallets are compared in Fig. 13 and Fig. 14 respectively.

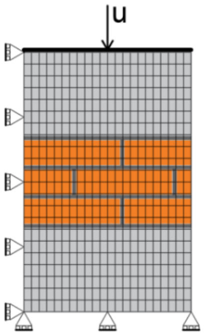

Fig. 11 – Boundary conditions and FEM mesh for combined masonry prisms

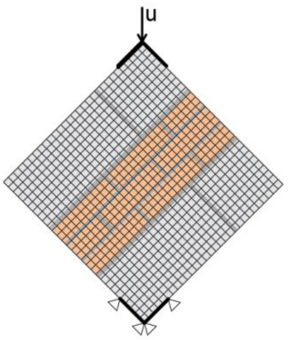

Fig. 12 – Boundary conditions and FEM mesh for combined masonry wallets

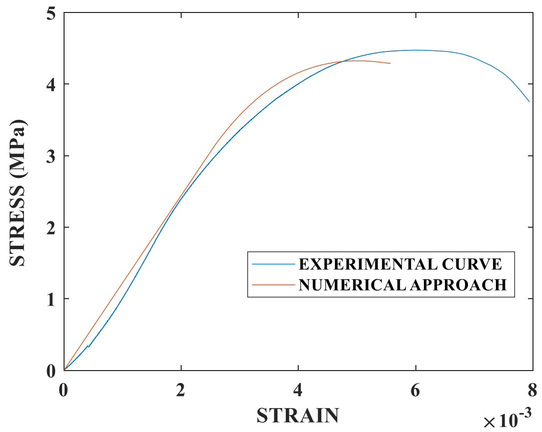

Fig. 13 – Stress – strain curves for combined masonry prisms

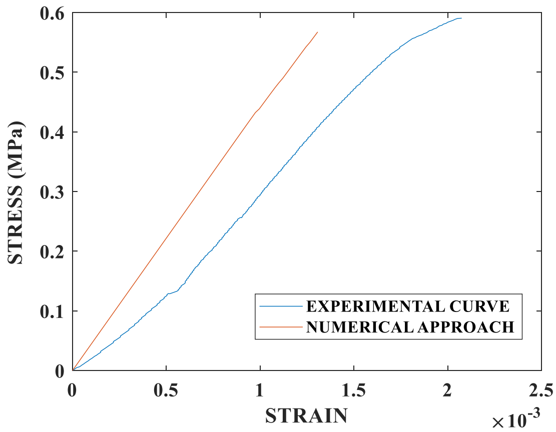

Fig. 14 – Curve stress – strain for combined masonry wallets

3.3 Numerical models of confined and combined masonry walls

For modeling confined and combined masonry walls, a micro-modeling was considered. In the micro-modeling, reinforced concrete confining elements were discretized by separate as an homogeneous material. For the combined masonry panel, blocks, bricks and mortar were modeled separately as homogeneous materials without considering a bonding-contact model between masonry units and mortar to simulate the debonding phenomena (Fig. 15). A lateral force was imposed on the top of the wall and restricted in its base and a pushover analyses was conducted. The stress contours for both principal directions are shown in Fig. 16. The final numerical configuration is depicted in Fig. 17a, where crack patterns are marked in yellow. The global story shear vs top displacement curve obtained with the micro-modeling is reported and compared to the experimental envelope in Fig. 18. It can be observed that the results are somewhat promising, but additional work is needed to try to capture the response envelope, as drifts are underestimated and load is overestimated, as the experimental response envelope was obtained from the cyclic testing of brittle materials that significantly deteriorate in stiffness and strength under cyclic loads, something that cannot be adequately represented in a pushover analysis of structural assemblages of these brittle materials. Therefore, numerical simulations using the applied cyclic loads is planned, to discern how useful this micro-modeling based upon Mazars' damage model is to represent such a complex heterogeneous structural element such as the studied confined and combined masonry walls under cyclic loading.

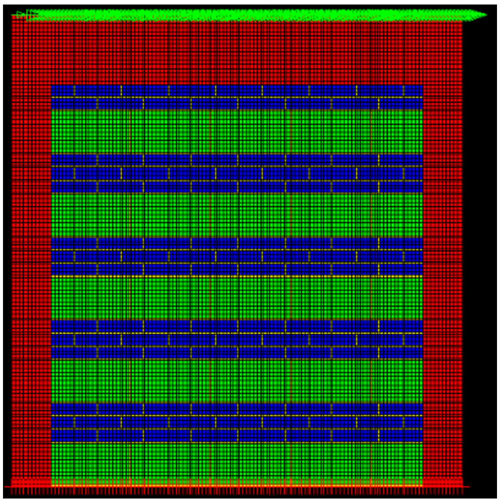

Fig. 15 – Mesh discretization for wall considering micro-modeling

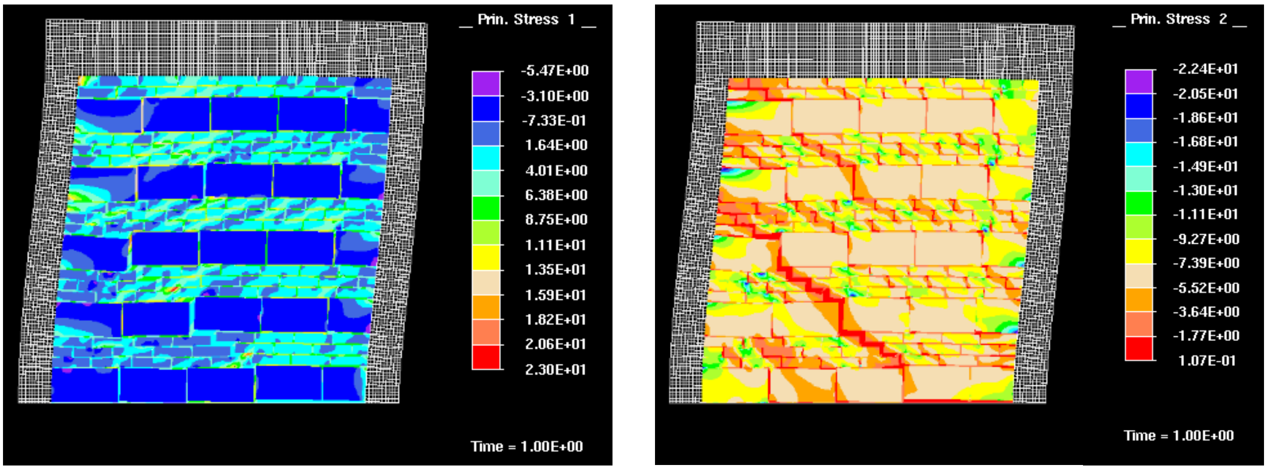

(a) (b)

Fig. 16 – Stress contour on the wall (a) Principal stress in direction "x", and (b) Principal stress in direction "y"

4. Conclusions

An integral experimental program which has been started was described in this paper, devoted to evaluate the cyclic behavior of combined and confined masonry walls, as well as the corresponding progress in numerical modeling. Experimental testing of masonry units, mortar, combined masonry prisms and wallets are reported, as well as the cyclic experimental testing of two confined and combined masonry walls.

For the numerical modeling, the mechanical damage model proposed originally by Mazars for concrete was implemented in the finite element software FEAP. For simplicity, this modeling has been initially employed to perform static nonlinear analyses of combined masonry prisms, wallets and combined and confined masonry walls, assuming a homogeneous modeling for masonry materials. The obtained numerical results were compared with experimental ones. From the obtained results to date, it can be concluded that there was a plausible correlation with experimental results for combined masonry prisms. Nevertheless, in the numerical models for combined masonry wallets there is certain variability among the numerical results with the experimental ones, as cyclic response has not been yet modeled numerically.

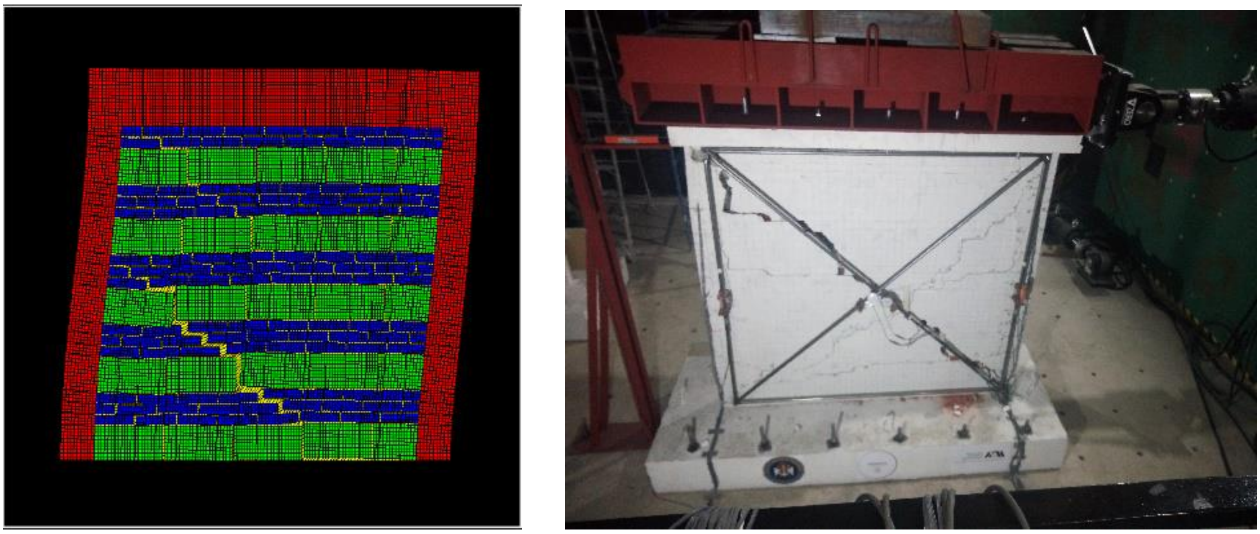

(a) Final numerical configuration. (b) Final cracking patterns of tested wall

Fig. 17 – Final numerical and experimental wall configuration.

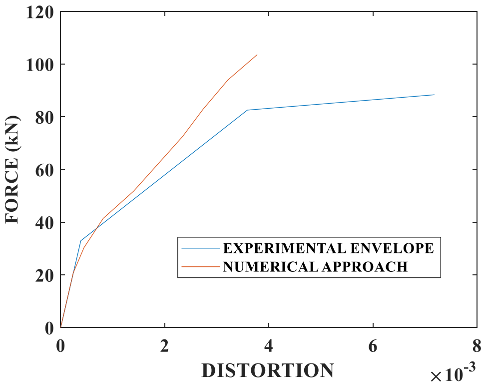

Fig. 18 – Comparison of experimental and numerical global response curves

Respect to numerical the numerical modeling to perform the static nonlinear response for complete confined and combined masonry walls, with the studied micro-modeling, a reasonable approximation is obtained at initial cracking and up to a drift of 0.3%, but after this drift the numerical curve overestimates the strength and underestimates deflections. This is due in part that a cyclic response envelope curve is compared with a pushover curve, where cyclic degradation in strength and stiffness is not correctly represented, particularly in brittle material such as those used in combined and confined masonry walls. Therefore, numerical simulations using the applied cyclic loads is planned, to discern how useful this micro-modeling based upon Mazars' damage model is to represent a complex heterogeneous structural element such as the studied confined and combined masonry walls. This is not an easy task, given all the numerical problems related using constitutive models with negative unloading stiffnesses in cyclic and dynamic simulations using refined finite element meshes. However, the authors are starting to work in that direction, and hopefully would be able to report the obtained results in the near future.

5. Acknowledgements

The experimental study was possible because of the enthusiastic collaboration of several colleagues, also by students at Engineering Military College from México, as well as Professors and technicians at Universidad Autónoma Metropolitana. Also for students and professors at Instituto Politécnico Nacional for their valuable assistance in the numerical work. The first author wants to acknowledge CONACYT for the financial support.

6. References

[1]. Quinteros RD, Bellomo F, Nallim LG, Oller S (2014): Modelo para el Análisis Estructural del Comportamiento de Mampostería Mediante Técnicas de Homogeneización. *Mecánica Computacional*, **Vol. XXXIII**, 1253-1269.
[2]. Tena-Colunga A, Juárez-Ángeles A, Salinas-Vallejo VH (2009): Cyclic behavior of combined and confined masonry walls. *Engineering Structures* **31** (1), 240-259.
[3]. Tena Colunga A (2018): Algunos aspectos a considerar en el modelado de estructuras para el análisis y diseño por sismo. *XXI Congreso Nacional de Ingeniería Estructural*, Campeche, Mexico.
[4]. NTCM-2017 (2017): *Normas Técnicas Complementarias para Diseño y Construcción de Estructuras de Mampostería*. Gaceta Oficial del Distrito Federal.
[5]. Comité Técnico de Normalización de Productos, Sistemas y Servicios para la Construcción (2013): *NMX-C-036-ONNCCE-2013. Industria de la construcción - Mampostería – Resistencia a la compresión de bloques, tabiques o ladrillos y tabicones y adoquines – Método de ensayo*. Organismo Nacional de Normalización y Certificación de la Construcción y la Edificación, S.C.
[6]. Comité Técnico de Normalización de Productos, Sistemas y Servicios para la Construcción (2014): *NMX-C-037-ONNCCE-2013. Industria de la construcción - Mampostería - Determinación de la absorción total y la absorción inicial de agua en bloques, tabiques o ladrillos y tabicones – Método de ensayo*. Organismo Nacional de Normalización y Certificación de la Construcción y la Edificación, S.C.
[7]. Comité Técnico de Normalización de Productos, Sistemas y Servicios para la Construcción (2011): *NMX-C-464-ONNCCE-2010. Industria de la construcción – Mampostería – Determinación de la resistencia de compresión diagonal y módulo de cortante de muretes, así como la determinación de la resistencia a compresión y módulo de elasticidad de pilas de mampostería de arcilla o de concreto - Métodos de ensayo*. Organismo Nacional de Normalización y Certificación de la Construcción y la Edificación, S.C.
[8]. Comité Técnico de Normalización de Productos, Sistemas y Servicios para la Construcción (2014): *NMX-C-486-ONNCCE-2014. Industria de la construcción – Mampostería - Mortero para uso estructural - Especificaciones y método de ensayo.* Organismo Nacional de Normalización y Certificación de la Construcción y la Edificación, S.C.
[9]. Comité Técnico de Normalización de Productos, Sistemas y Servicios para la Construcción (2014): *NMX-C-082-ONNCCE-2013, Industria de la construcción-mampostería-determinación de la adherencia por esfuerzo cortante entre el mortero y las piezas de mampostería -método de ensayo*. Organismo Nacional de Normalización y Certificación de la Construcción y la Edificación, S.C.
[10]. Popovics S (1973): A numerical approach to the complete stress-strain curve of concrete. *Cement and concrete research*, **Vol. 3**, 583-599.
[11]. Mazars JM, Pijaudier-Cabot G (1989): Continuum damage theory. Application to concrete. *Journal of Engineering Mechanics*, **115** (2), 345- 365.
[12]. Taylor RL (2001): FEAP - A Finite Element Analysis Program. *User Manual (Ver. 7.3)*. University of California, Berkeley, USA.
[13]. Hamon F (2013): Modèle d'endommagement de Mazars. *Code_Aster documentation. Clé R7.01.08*, Electricite de France Research and Development, Paris, France.
[14]. Betti M, Bartoli G, Corazzi R, Kovačević V (2015): Engineer Education and Research With Code Aster. *Conference: WEEF2015: World Engineering Education Forum*, Florence, Italy.

